The patatin-like phospholipase domain-containing 3 148M variant exacerbates alcohol-induced liver injury and tumorigenesis in mice

Jung-Hyo Cho[1,2,#], **Hyeong-Geug Kim**[1,#], **Menghao Huang**[1,3,4], **Shen Wang**[1], **Sheng Liu**[4,5], **Alex Lu**[6], **Kyle McCrocklin**[7], **Yang Zhang**[1], **Zhigang Fang**[1], **Juexin Wang**[7,8], **Wanqing Liu**[9], **Jun Wan**[4,5,7,8], **X. Charlie Dong**[1,3,5,7,8,*]

[1]Department of Biochemistry and Molecular Biology, School of Medicine, Indiana University, Indianapolis, IN 46202, USA

[2]Department of East & West Cancer Center, Daejeon Korean Medicine Hospital of Daejeon University, 75, Daedeok-daero 176, Seo-gu, Daejeon 35235, Korea

[3]Center for Diabetes and Metabolic Diseases, Indiana University, Indianapolis, IN 46202, USA

[4]Melvin and Bren Simon Comprehensive Cancer Center, Indiana University, Indianapolis, IN 46202, USA

[5]Department of Medical and Molecular Genetics, School of Medicine, Indiana University, Indianapolis, IN 46202, USA

[6]Park Tudor School, Indianapolis, IN 46240, USA

[7]Luddy School of Informatics, Computing, and Engineering, Indiana University, Indianapolis, IN 46202, USA

[8]Center for Computational Biology and Bioinformatics, School of Medicine, Indiana University, Indianapolis, IN 46202, USA

[9]Department of Pharmaceutical Sciences, Eugene Applebaum College of Pharmacy and Health Sciences, Wayne State University, Detroit, MI 48201, USA

Abstract

Patatin-like phospholipase domain–containing 3 (PNPLA3) protein 148M variant is strongly associated with cirrhosis and hepatocellular carcinoma (HCC); however, the underlying mechanisms remain elusive. This study aimed to elucidate the role of the PNPLA3^{148M} variant in the alcohol-related HCC development. Control and humanized PNPLA3^{148M} transgenic mice were fed with an ethanol-containing diet for 12 weeks. The animals were examined for liver

[*]Corresponding author: Department of Biochemistry and Molecular Biology, School of Medicine, Indiana University, Indianapolis, IN 46202, USA. xcdong@iu.edu.

Author contributions: JHC and HGK performed experiments and wrote the manuscript; MH performed experiments; SW performed experiments; SL performed data analysis; AL performed experiments; KM, performed data analysis; YZ performed experiments; ZF performed experiments; JXW, performed data analysis and data interpretation; WL contributed to the animal model development; JW performed data analysis and interpretation; XCD performed experimental design and data analysis and wrote the manuscript.

[#]These authors contributed equally.

Conflict of interest statement: None.

tumors. After the alcohol feeding, the PNPLA3^{148M} mice had 2-fold higher liver cancer incidence rates and larger tumor sizes than that in the control mice. Cancer stem cell markers in the PNPLA3^{148M} mouse livers were elevated relative to that in the control mouse livers. Alcohol detoxification was impaired in the PNPLA3^{148M} mouse livers. Hepatic oxidative stress and DNA damage were elevated in the PNPLA3^{148M} mice. Wnt/β-catenin and Yes-associated protein (YAP) and WW domain containing transcription regulator 1 (WWTR1/TAZ) were activated in the PNPLA3^{148M} mouse livers. Our data suggest that the PNPLA3^{148M} variant has a strong interaction with alcohol in the HCC development through attenuation of alcohol detoxification and promotion of oncogenic pathways. Targeting the PNPLA3^{148M} variant might be useful for the prevention or treatment of alcohol-associated HCC in patients carrying this variant.

Introduction

Alcohol use has been a significant risk factor for human morbidity and mortality in the world. A report has shown that approximately 3 million deaths were associated with alcohol use in 2016 alone [1]. Alcohol is a common cause of liver diseases ranging from hepatic steatosis, hepatitis, cirrhosis, and hepatocellular carcinoma (HCC). HCC is a predominant form of liver cancer that is a leading cause of cancer deaths worldwide. A recent study of Chinese patients with alcohol-associated liver disease (ALD) has revealed a marked increase in ALD-associated HCC from 5.8% to 30.7% between 2002 and 2018 [2]. Ethanol is classified as a group 1 human carcinogen by the International Agency for Research on Cancer; however, how ethanol causes cancer is not fully understood. Ethanol is primarily metabolized in the liver by two key enzymes – alcohol dehydrogenase (ADH) and aldehyde dehydrogenase (ALDH). ADH catalyzes the first reaction from ethanol to acetaldehyde, which is highly reactive and can form adducts with proteins and DNAs [3]. Under normal conditions, acetaldehyde is rapidly converted to acetate by ALDH. ALDH2 is the predominant ALDH in the liver [4].

Numerous genes and pathways have been implicated in the HCC development. Among them, the Wnt/β-catenin and the Hippo pathways play a significant role in HCC tumorigenesis [5]. In the absence of Wnt ligands, β-catenin (CTNNB1) is cytosolic and subject to ubiquitin-mediated degradation. Upon Wnt ligands binding to the Frizzled receptors, β-catenin is skipped from degradation and translocated to the nucleus for transcriptional function. It has been suggested that 30-40% HCC tumors have aberrant activation of the Wnt/β-catenin pathway [5]. For the Hippo pathway, Yes-associated protein (YAP) and WW domain containing transcription regulator 1 (WWTR1, also commonly known as TAZ) are two major downstream effectors [6]. When the Hippo signaling is on, YAP and TAZ can be phosphorylated by large tumor suppressor 1/2 (LATS1/2) and subject to proteasomal degradation. When the Hippo signaling is off, non-phosphorylated YAP/TAZ can be translocated to the nucleus and coactivate TEA domain transcription factors (TEAD1-4). In HCC, YAP is generally not mutated, instead, gene amplification and post-translational modifications lead to elevated YAP protein levels [7].

Numerous genome-wide association studies have identified a single nucleotide polymorphism (rs738409, C→G) in the human patatin-like phospholipase domain-containing protein 3 (PNPLA3) gene, which results in isoleucine (I) to methionine (M) substitution at amino acid 148, as the most significant gene variant for the alcohol-related cirrhosis and HCC [8–10]. The PNPLA3^{148M} variant is associated with 2-3 fold higher risk for alcohol-related cirrhosis and 2-4 fold higher risk for alcohol-related HCC in carriers than non-carriers, respectively [8–10]. PNPLA3 is a lipid droplet-associated protein that is highly abundant in human livers. Biochemical studies have shown that PNPLA3 has triglyceride lipase and retinyl palmitate hydrolase activities; however, the pathophysiological function of the PNPLA3^{148M} variant remains elusive [11]. In this study, we used humanized PNPLA3 transgenic mouse models to investigate the role of the PNPLA3^{148M} variant in alcohol-related HCC pathogenesis.

Materials and Methods

Animals.

Human PNPLA3^{148I} and PNPLA3^{148M} transgenic mice were generated using a human bacterial artificial clone harboring the human *PNPLA3* gene and mutagenesis for creation of the PNPLA3^{148M} variant as we previously reported [12]. The transgenic mice were on the C57BL/6 genetic background. An HCC mouse model was generated by cotreatment with a 5% (vol/vol) of ethanol diet (Lieber-DeCarli diet, Bio-Serv, Flemington, NJ) and CCl_4. Briefly, wild-type (WT), PNPLA3^{148I}, and PNPLA3^{148M} mice were first acclimated to the ethanol-containing liquid diet by a gradual increase (1% per day) in ethanol concentration from 0% to 5% (vol/vol) during the first six days and then treated with the 5% ethanol (vol/vol) diet for 12 weeks. In the same time, the animals were intraperitoneally injected with CCl_4 in corn oil weekly at a dose of 0.32 µg/g of body weight for 10 weeks. At the end of experiment, the animals were euthanized for blood and tissue sample collections.

Histological analysis.

Tissue samples were fixed in 10% formalin, embedded, sectioned, and stained with hematoxylin and eosin (H&E) at the Histology Core of Indiana University School of Medicine. For immunofluorescence (IF) analysis, tissue sections were processed as we previously reported [13]. The antibodies used in this work: alpha fetoprotein (AFP, Santa Cruz Biotechnology sc-8399), arginase 1 (ARG1, Cell Signaling Technology #93668S), CD44 molecule (CD44, Santa Cruz Biotechnology sc-7297), CD133 (Novus Biologicals NBP2-44250), 4-hydroxynonenal (4-HNE, R&D Systems MAB-3249), malondialdehyde (MDA, Thermo Fisher Scientific MA5-27560), pH2A.X (Cell Signaling Technology #9718S), tumor protein P53 binding protein 1 (TP53BP1, Bethyl Labs A300-272A-M), collagen 1 (COL1, Abcam ab260043), collagen 3 (COL3, Abcam ab7778), smooth muscle actin alpha 2 (ACTA2, Abcam ab5694), TIMP metallopeptidase inhibitor 1 (TIMP1, Proteintech #10753-1-AP), WNT4 (Santa Cruz Biotechnology sc-376279), CTNNB1 (Cell Signaling Technology #8480S), YAP (Cell Signaling Technology #14074S), TAZ/WWTR1 (Cell Signaling Technology #82630S). IF images were taken using a Zeiss fluorescence microscope with an AxionVison Rel 4.8 software. Images were analyzed using ImageJ (Version 1.54, February 18, 2025, https://imagej.net/ij/download.html, National Institutes of Health, Bethesda, MD).

Biochemical analysis.

Measurements of acetaldehyde, hydrogen peroxide, nitric oxide, MDA, and glutathione in liver tissue samples were performed using commercial kits from BioAssay Systems (Hayward, CA), Thermo Fisher Scientific (Waltham, MA), Abcam (Waltham, MA), and Sigma-Aldrich (St. Louis, MO), respectively as previously described [13].

Protein analysis.

Mouse tissue samples were homogenized using a T25 digital homogenizer (IKA Works Inc., Wilmington, NC) in lysis buffer (50 mM HEPES, pH 7.5, 150 mM NaCl, 10% Glycerol, 1% Triton X-100, 1.5 mM $MgCl_2$, 1 mM EDTA, 10 mM sodium pyrophosphate, 100 mM sodium fluoride, 100 μM sodium vanadate, 1 mM PMSF and Complete Protease Inhibitor (Sigma-Aldrich). Protein samples were resolved by 10% sodium dodecyl sulfate polyacrylamide gel electrophoresis and transferred to a nitrocellulose membrane using a Trans-Blot Turbo Transfer System (Bio-Rad Laboratories, Hercules, CA). Membranes were first incubated with a blocking buffer and then with specific primary antibodies overnight at 4 °C. Some of the antibodies used for immunostaining were also used for immunoblotting. Other antibodies used were described in the following: PNPLA3 (Thermo Fisher Scientific #PA5-18901), perilipin 2 (PLIN2, Proteintech #A6276), ALDH2 (Thermo Fisher Scientific MA5-17029), actinin alpha (ACTN, Santa Cruz Biotechnology sc-17829), and actin beta (ACTB, Abcam ab8226). After three washes with Tris-buffered saline solution containing 0.1% Tween-20, membranes were incubated with horseradish peroxidase conjugated secondary antibodies at a dilution of 1:1000 (Cell Signaling Technology, Danvers, MA) for 1 h at room temperature. Signals were detected using enhanced chemiluminescence substrates (Thermo Fisher Scientific) and imaged on a ChemiDoc MP Imaging System (Bio-Rad Laboratories). Images were analyzed using the ImageJ software.

RNA analysis.

Total RNAs were extracted and purified from mouse tissue samples using TRI Reagent (Sigma-Aldrich) and cDNA was synthesized using a High-Capacity cDNA Reverse Transcription Kit (Thermo Fisher Scientific) according to the manufacturer's instruction. Real-time PCR was performed using an Eppendorf Realplex PCR system with specific primers described in Table 1 and SYBR Green PCR Master Mix (Thermo Fisher Scientific). Expression of a target gene of interest relative to an internal control gene peptidylprolyl isomerase A (*Ppia*) was analyzed using the $2^{-\Delta\Delta Ct}$ method.

Statistical analysis.

Data were presented as mean ± standard error (SEM). Comparisons between two groups were analyzed using non-parametric Mann-Whitney tests. Comparisons among multiple groups were performed using non-parametric Kruskal-Wallis tests (Prism version 10.2.1, GraphPad, La Jolla, CA).

Results

The PNPLA3^{148M} variant exacerbates alcohol-related HCC development.

As reported previously [12], we generated transgenic mice carrying human PNPLA3^{148I} and PNPLA3^{148M} genomic sequences. Expression of human PNPLA3 protein in the transgenic mouse livers was verified by Western blot analysis of hepatic lipid droplet protein lysates (Fig. 1A). The line #1 PNPLA3^{148I} and line #2 PNPLA3^{148M} transgenic mice were used for this study as they had comparable overexpression. To develop an ethanol-related HCC mouse model, we treated WT, PNPLA3^{148I} and PNPLA3^{148M} mice with a liquid diet containing 5% ethanol (vol/vol) for 12 weeks plus weekly CCl_4 injections for 10 weeks (Fig. 1B). At the end of the experiment, body weights of the PNPLA3^{148M} mice were not significantly different from the WT mice but significantly less than that of the PNPLA3^{148I} mice whereas there was no significant difference in liver weights among three groups of mice (Fig. 1 C–E). However, liver cancer phenotype was strikingly different (Fig. 1F). Liver cancer incidence rates were 33.3%, 0%, and 85.7% in WT, PNPLA3^{148I} and PNPLA3^{148M} mice, respectively (Fig. 1G). Liver tumors were more and bigger in the PNPLA3^{148M} mice than that in the WT mice (Fig. 1 H, I). As expected, hepatic steatosis was significantly elevated in the the PNPLA3^{148M} mice compared to the WT and PNPLA3^{148I} mice (Fig. 2 A, B). Tumor marker analysis confirmed worse HCC in the PNPLA3^{148M} mice as AFP, ARG1, CD44, and CD133 protein levels were significantly higher in the liver sections of the PNPLA3^{148M} mice than that in the WT or PNPLA3^{148I} mice (Fig. 2 C, D). Cell proliferation rates were also significantly increased in the the PNPLA3^{148M} mouse livers compared to the WT and PNPLA3^{148I} mouse livers (Fig. 3 A–C).

PNPLA3^{148M} impairs ethanol detoxification and exacerbates oxidative stress.

To examine how the PNPLA3^{148M} variant impacts on ethanol-induced liver injury, we first analyzed a key ethanol-detoxification enzyme ALDH2 at both protein and mRNA levels. ALDH2 expression was increased in the liver of PNPLA3^{148I} mice but decreased in the liver of PNPLA3^{148M} mice (Fig. 4 A–C). As a result, hepatic acetaldehyde levels were significantly elevated in the PNPLA3^{148M} mice (Fig. 4D). In addition, Adh1 and Adh4 mRNA levels were also significantly decreased in the in the liver of PNPLA3^{148M} mice (Fig. 4E). Next, we analyzed reactive oxygen species (ROS) and DNA damage in the liver of ethanol-treated mice. Fluorescence intensities of dichlorodihydrofluorescein diacetate (DCFDA, a probe for H_2O_2), dihydroethidium (DHE, a probe for superoxide and H_2O_2), malondialdehyde (MDA), phospho-histone H2A.X (pH2A.X) at Ser139, and TP53BP1 were significantly elevated in the liver of the PNPLA3^{148M} mice compared to WT and PNPLA3^{148I} mice (Fig. 5 A, B). Biochemical analysis confirmed an increase in H_2O_2, nitric oxide (NO), MDA in the liver of the PNPLA3^{148M} mice compared to WT and PNPLA3^{148I} mice whereas hepatic total glutathione levels were not significantly different among three groups of mice (Fig. 5 C–F).

Hepatic fibrosis is comparable between the PNPLA3^{148I} and PNPLA3^{148M} mice.

As PNPLA3^{148M} has been previously implicated in hepatic fibrosis [14–20], we also analyzed several fibrosis markers in the liver by immunofluorescence imaging and immunoblotting. Our data showed that expression of COL1, COL3, ACTA2, and TIMP1 was higher in the liver of WT mice than that in the PNPLA3^{148I} and PNPLA3^{148M} mice (Fig. 6 A–D). This suggests that hepatic fibrosis might not be a major driver for the ethanol-induced HCC in the PNPLA3^{148M} mice.

Wnt and β-catenin are elevated in the PNPLA3^{148M} mouse liver

As β-catenin is often involved in the HCC development, we analyzed expression of β-catenin and Wnt ligands. Our data showed that Ctnnb1 and Wnt family members 4 and 5b (Wnt4 and Wnt5b) mRNAs were elevated in the liver of PNPLA3^{148M} mice compared to WT and PNPLA3^{148I} mice (Fig. 7 A, B). Immunoblot analysis also showed a trend of increase in β-catenin protein levels (Fig. 7 C, D). Immunofluorescence analysis confirmed an increase in WNT4 and β-catenin proteins in the PNPLA3^{148M} mouse livers (Fig. 7 E, F).

The Hippo signaling pathway is dysregulated in the PNPLA3^{148M} mouse liver

Next, we analyzed key factors in the downstream of the Hippo signaling pathway. Immunoblot analysis showed that phosphorylated YAP (Ser127) levels trended down whereas TAZ and TEAD1 protein levels trended up (Fig. 8 A, B). Immunofluorescence analysis also showed that YAP and TAZ had increased nuclear translocation in the PNPLA3^{148M} mouse livers (Fig. 8 C–E). As a result, expression of the Hippo downstream target genes cysteine-rich angiogenic inducer (*Cyr61*, also named *Ccn1)* and connective tissue growth factor (*Ctgf,* also named *Ccn2*) trended up in the liver of the PNPLA3^{148M} mice (Fig. 8 F, G). In addition, expression of the *Tet* methylcytosine dioxygenase genes was also increased (Fig. 8H), which is consistent with a previous report suggesting that *Tet1* is a YAP target gene [21].

Discussion

In this work, we have illustrated a significant role of the PNPLA3^{148M} variant in the development of alcohol-related HCC. Previously, the PNPLA3^{148M} variant has been associated with alcohol-related cirrhosis and HCC in multiple human cohort studies [8–10]. Now our data have provided some potential molecular links to the HCC development. First, PNPLA3^{148M} hepatocytes have attenuated alcohol detoxification function as ALDH2 is decreased and acetaldehyde is increased in the PNPLA3^{148M} mouse liver. This is consistent with the previous reports suggesting that ALDH2 deficiency increases the risk of HCC development in human patients with cirrhosis and ALD and an ALD plus CCl_4 mouse model as well [22, 23]. Second, reactive oxygen species are elevated in the PNPLA3^{148M} mouse liver. As a result, biomolecules including lipids, proteins, and DNAs may be damaged by free radicals. It is likely that DNA damage could lead to oncogenic mutations and/or dysregulation. Third, key oncogenic pathways including Wnt/β-catenin and the Hippo pathway are dysregulated in the PNPLA3^{148M} mouse liver. Those alterations could promote HCC initiation and progression. Collectively, those alterations significantly increase the risk of HCC development through the interaction between the PNPLA3^{148M} variant and alcohol metabolism. It is worth noting that mutation of the corresponding 148I to 148M in the mouse *Pnpla3* gene does not lead to HCC development in mice under either chow or Western diet plus 10% (vol/vol) ethanol and 23.1 g/L fructose and 18.9 g/L glucose in the drinking water for up to 50 weeks [24]. The differential phenotypes could be attributed to multiple factors including human versus mouse *Pnpla3* gene [11], experimental design, and animal housing facility.

As PNPLA3 is a lipid droplet-associated protein, lipid droplet metabolism could play a role in the PNPLA3^{148M} variant-associated HCC [11]. This seems consistent with the histology of the liver tumors in the PNPLA3^{148M} mice. Previously, it has been suggested that PNPLA3^{148M} sequesters abhydrolase domain containing 5 (ABHD5 or commonly known as CGI-58) from PNPLA2 (commonly known as ATGL for adipose triglyceride lipase) and thus decreases lipolysis [25]. Intriguingly, we have observed that alcohol metabolism is also impaired by the PNPLA3^{148M} variant, especially accumulation of acetaldehyde. This could partially explain the elevated risk of HCC in the PNPLA3^{148M} mice. But there is another twist. Hepatic fibrosis is not exacerbated by the PNPLA3^{148M} variant under the alcohol feeding and tetrachloride treatment conditions even though PNPLA3^{148M} has been shown to promote hepatic stellate cell activation in vitro [14].

Somatic mutations of the *CTNNB1* gene, coding for β-catenin, have been found in nearly 50% patients with alcohol-related HCC [5]. A genome-wide association analysis has identified a protective WNT3A-WNT9A rs708113[T] allele in alcohol-related HCC cohorts. Interestingly, this protective allele is associated with HCC tumors with a lower rate of *CTNNB1* somatic mutations. Further analysis suggests that the rs708113[T] allele might enhance tumor immune response in the non-tumor liver tissue [26]. In this study, our data suggest that PNPLA3^{148M} activates the Wnt/β-catenin pathway partly by increasing both Wnt ligands and nuclear β-catenin. But it is still elusive how PNPLA3^{148M} does that. As PNPLA3 is normally localized on lipid droplet, it is reasonable to believe that the Wnt/β-catenin pathway is indirectly regulated by PNPLA3^{148M}.

The Hippo pathway has been implicated in the liver cancer development [27–43]; however, it is unclear whether this is the case for alcohol-related HCC. Our data have shown that YAP, TAZ, and TEAD1 in the downstream of the Hippo pathway are elevated in the PNPLA3^{148M} mouse livers, suggesting that the Hippo pathway is indeed involved in the alcohol-related HCC. Previously, it has been reported that YAP is activated by PNPLA3^{148M} in human hepatic stellate cells [44]. However, it is unclear how the Hippo pathway is regulated by PNPLA3^{148M} and whether this occurs in the early or late stage of the HCC development. Additional studies are needed to address those questions.

It is generally believed that HCC originates from dedifferentiated hepatocytes that may express cancer stem cell markers such as CD44 and CD133 [45, 46]. The PNPLA3^{148M} mouse livers exhibit elevated these markers. Lineage tracing approaches would be useful to track whether those CD44$^+$ or CD133$^+$ cells are the initiating cells for HCC. Apparently, PNPLA3^{148M} increases the number of those cells under the alcohol and CCl_4 conditions. It would be interesting to illustrate the role of PNPLA3^{148M} in the generation of those potential HCC initiating cells.

In summary, this study has shown an elevated risk for alcohol-related HCC in PNPLA3^{148M} variant carriers. PNPLA3^{148M} impairs alcohol detoxification and increases hepatic oxidative stress and DNA damage. The Wnt/β-catenin and YAP/TAZ pathways are activated in the

PNPLA3^{148M} livers. These findings suggest that PNPLA3 can be targeted for the prevention or treatment of alcohol-associated HCC in PNPLA3^{148M} variant carriers.

Acknowledgements

We thank Dr. Xiongbin Lu for the scientific discussion and useful advice, and Rachel Schweiger, Dr. Jiazhi Xu and Dr. Lu Wang for the excellent technical assistance.

Funding:

This work was supported in part by the National Institute of Diabetes and Digestive and Kidney Diseases (R01DK121925, R01DK120689, R01DK124612, P30DK097512), the National Institute on Alcohol Abuse and Alcoholism (R01AA028506 and UT2AA031151), the National Institute on Aging (R21AG072288), and the Heartland Children's Nutrition Collaborative Fund at Riley Children's Foundation.

References

[1]. Huang DQ, Mathurin P, Cortez-Pinto H, Loomba R: Global epidemiology of alcohol-associated cirrhosis and HCC: trends, projections and risk factors. Nat Rev Gastroenterol Hepatol 2023, 20:37–49. [PubMed: 36258033]

[2]. Chang B, Tian H, Huang A, Zhai X, Wang Q, Han L, Jin X, Gao L, Liang Q, Li B, Lu Y, Xie H, Ji D, Zou Z: Prevalence and prediction of hepatocellular carcinoma in alcohol-associated liver disease: a retrospective study of 136 571 patients with chronic liver diseases. eGastroenterology 2024, 2:e100036. [PubMed: 39944749]

[3]. Gao H, Jiang Y, Zeng G, Huda N, Thoudam T, Yang Z, Liangpunsakul S, Ma J: Cell-to-cell and organ-to-organ crosstalk in the pathogenesis of alcohol-associated liver disease. eGastroenterology 2024, 2.

[4]. Rodriguez FD, Covenas R: Biochemical Mechanisms Associating Alcohol Use Disorders with Cancers. Cancers (Basel) 2021, 13.

[5]. Xu C, Xu Z, Zhang Y, Evert M, Calvisi DF, Chen X: beta-Catenin signaling in hepatocellular carcinoma. J Clin Invest 2022, 132.

[6]. Driskill JH, Pan D: The Hippo Pathway in Liver Homeostasis and Pathophysiology. Annu Rev Pathol 2020.

[7]. Patel SH, Camargo FD, Yimlamai D: Hippo Signaling in the Liver Regulates Organ Size, Cell Fate, and Carcinogenesis. Gastroenterology 2017, 152:533–45. [PubMed: 28003097]

[8]. Buch S, Stickel F, Trepo E, Way M, Herrmann A, Nischalke HD, Brosch M, Rosendahl J, Berg T, Ridinger M, Rietschel M, McQuillin A, Frank J, Kiefer F, Schreiber S, Lieb W, Soyka M, Semmo N, Aigner E, Datz C, Schmelz R, Bruckner S, Zeissig S, Stephan AM, Wodarz N, Deviere J, Clumeck N, Sarrazin C, Lammert F, Gustot T, Deltenre P, Volzke H, Lerch MM, Mayerle J, Eyer F, Schafmayer C, Cichon S, Nothen MM, Nothnagel M, Ellinghaus D, Huse K, Franke A, Zopf S, Hellerbrand C, Moreno C, Franchimont D, Morgan MY, Hampe J: A genome-wide association study confirms PNPLA3 and identifies TM6SF2 and MBOAT7 as risk loci for alcohol-related cirrhosis. Nat Genet 2015, 47:1443–8. [PubMed: 26482880]

[9]. Falleti E, Cussigh A, Cmet S, Fabris C, Toniutto P: PNPLA3 rs738409 and TM6SF2 rs58542926 variants increase the risk of hepatocellular carcinoma in alcoholic cirrhosis. Digestive and liver disease : official journal of the Italian Society of Gastroenterology and the Italian Association for the Study of the Liver 2016, 48:69–75. [PubMed: 26493626]

[10]. Trepo E, Guyot E, Ganne-Carrie N, Degre D, Gustot T, Franchimont D, Sutton A, Nahon P, Moreno C: PNPLA3 (rs738409 C>G) is a common risk variant associated with hepatocellular carcinoma in alcoholic cirrhosis. Hepatology 2012, 55:1307–8. [PubMed: 22162034]

[11]. Dong XC: PNPLA3-A Potential Therapeutic Target for Personalized Treatment of Chronic Liver Disease. Front Med (Lausanne) 2019, 6:304. [PubMed: 31921875]

[12]. Liu Z, Zhang Y, Graham S, Wang X, Cai D, Huang M, Pique-Regi R, Dong XC, Chen YE, Willer C, Liu W: Causal relationships between NAFLD, T2D and obesity have implications for disease subphenotyping. J Hepatol 2020, 73:263–76. [PubMed: 32165250]

[13]. Fang Z, Kim HG, Huang M, Chowdhury K, Li MO, Liangpunsakul S, Dong XC: Sestrin Proteins Protect Against Lipotoxicity-Induced Oxidative Stress in the Liver via Suppression of C-Jun N-Terminal Kinases. Cell Mol Gastroenterol Hepatol 2021, 12:921–42. [PubMed: 33962074]

[14]. Bruschi FV, Claudel T, Tardelli M, Caligiuri A, Stulnig TM, Marra F, Trauner M: The PNPLA3 I148M variant modulates the fibrogenic phenotype of human hepatic stellate cells. Hepatology 2017, 65:1875–90. [PubMed: 28073161]

[15]. Lee SS, Byoun YS, Jeong SH, Woo BH, Jang ES, Kim JW, Kim HY: Role of the PNPLA3 I148M polymorphism in nonalcoholic fatty liver disease and fibrosis in Korea. Dig Dis Sci 2014, 59:2967–74. [PubMed: 25069572]

[16]. Trepo E, Pradat P, Potthoff A, Momozawa Y, Quertinmont E, Gustot T, Lemmers A, Berthillon P, Amininejad L, Chevallier M, Schlue J, Kreipe H, Deviere J, Manns M, Trepo C, Sninsky J, Wedemeyer H, Franchimont D, Moreno C: Impact of patatin-like phospholipase-3 (rs738409 C>G) polymorphism on fibrosis progression and steatosis in chronic hepatitis C. Hepatology 2011, 54:60–9. [PubMed: 21488075]

[17]. Valenti L, Al-Serri A, Daly AK, Galmozzi E, Rametta R, Dongiovanni P, Nobili V, Mozzi E, Roviaro G, Vanni E, Bugianesi E, Maggioni M, Fracanzani AL, Fargion S, Day CP: Homozygosity for the patatin-like phospholipase-3/adiponutrin I148M polymorphism influences liver fibrosis in patients with nonalcoholic fatty liver disease. Hepatology 2010, 51:1209–17. [PubMed: 20373368]

[18]. Pingitore P, Dongiovanni P, Motta BM, Meroni M, Lepore SM, Mancina RM, Pelusi S, Russo C, Caddeo A, Rossi G, Montalcini T, Pujia A, Wiklund O, Valenti L, Romeo S: PNPLA3 overexpression results in reduction of proteins predisposing to fibrosis. Hum Mol Genet 2016, 25:5212–22. [PubMed: 27742777]

[19]. Linden D, Ahnmark A, Pingitore P, Ciociola E, Ahlstedt I, Andreasson AC, Sasidharan K, Madeyski-Bengtson K, Zurek M, Mancina RM, Lindblom A, Bjursell M, Bottcher G, Stahlman M, Bohlooly YM, Haynes WG, Carlsson B, Graham M, Lee R, Murray S, Valenti L, Bhanot S, Akerblad P, Romeo S: Pnpla3 silencing with antisense oligonucleotides ameliorates nonalcoholic steatohepatitis and fibrosis in Pnpla3 I148M knock-in mice. Molecular metabolism 2019, 22:49–61. [PubMed: 30772256]

[20]. Scheiner B, Mandorfer M, Schwabl P, Payer BA, Bucsics T, Bota S, Aichelburg MC, Grabmeier-Pfistershammer K, Stattermayer A, Ferenci P, Trauner M, Peck-Radosavljevic M, Reiberger T: The Impact of PNPLA3 rs738409 SNP on Liver Fibrosis Progression, Portal Hypertension and Hepatic Steatosis in HIV/HCV Coinfection. PLoS One 2015, 10:e0143429. [PubMed: 26599080]

[21]. Wu BK, Mei SC, Chen EH, Zheng Y, Pan D: YAP induces an oncogenic transcriptional program through TET1-mediated epigenetic remodeling in liver growth and tumorigenesis. Nat Genet 2022, 54:1202–13. [PubMed: 35835915]

[22]. Seo W, Gao Y, He Y, Sun J, Xu H, Feng D, Park SH, Cho YE, Guillot A, Ren T, Wu R, Wang J, Kim SJ, Hwang S, Liangpunsakul S, Yang Y, Niu J, Gao B: ALDH2 deficiency promotes alcohol-associated liver cancer by activating oncogenic pathways via oxidized DNA-enriched extracellular vesicles. J Hepatol 2019, 71:1000–11. [PubMed: 31279903]

[23]. Wen Y, Ma L, Ju C: Recent insights into the pathogenesis and therapeutic targets of chronic liver diseases. eGastroenterology 2023, 1.

[24]. Patsenker E, Thangapandi VR, Knittelfelder O, Palladini A, Hefti M, Beil-Wagner J, Rogler G, Buch T, Shevchenko A, Hampe J, Stickel F: The PNPLA3 variant I148M reveals protective effects toward hepatocellular carcinoma in mice via restoration of omega-3 polyunsaturated fats. J Nutr Biochem 2022, 108:109081. [PubMed: 35691594]

[25]. Wang Y, Kory N, BasuRay S, Cohen JC, Hobbs HH: PNPLA3, CGI-58, and Inhibition of Hepatic Triglyceride Hydrolysis in Mice. Hepatology 2019, 69:2427–41. [PubMed: 30802989]

[26]. Trepo E, Caruso S, Yang J, Imbeaud S, Couchy G, Bayard Q, Letouze E, Ganne-Carrie N, Moreno C, Oussalah A, Feray C, Blanc JF, Clement B, Hillon P, Boursier J, Paradis V, Calderaro J, Gnemmi V, Nault JC, Gueant JL, Deviere J, Archambeaud I, Vitellius C, Turlin B, Bronowicki JP, Gustot T, Sutton A, Consortium G, Ziol M, Nahon P, Zucman-Rossi J: Common genetic variation in alcohol-related hepatocellular carcinoma: a case-control genome-wide association study. Lancet Oncol 2022, 23:161–71. [PubMed: 34902334]

[27]. Zhou D, Conrad C, Xia F, Park JS, Payer B, Yin Y, Lauwers GY, Thasler W, Lee JT, Avruch J, Bardeesy N: Mst1 and Mst2 maintain hepatocyte quiescence and suppress hepatocellular carcinoma development through inactivation of the Yap1 oncogene. Cancer Cell 2009, 16:425–38. [PubMed: 19878874]

[28]. Lee KP, Lee JH, Kim TS, Kim TH, Park HD, Byun JS, Kim MC, Jeong WI, Calvisi DF, Kim JM, Lim DS: The Hippo-Salvador pathway restrains hepatic oval cell proliferation, liver size, and liver tumorigenesis. Proc Natl Acad Sci U S A 2010, 107:8248–53. [PubMed: 20404163]

[29]. Lu L, Li Y, Kim SM, Bossuyt W, Liu P, Qiu Q, Wang Y, Halder G, Finegold MJ, Lee JS, Johnson RL: Hippo signaling is a potent in vivo growth and tumor suppressor pathway in the mammalian liver. Proc Natl Acad Sci U S A 2010, 107:1437–42. [PubMed: 20080689]

[30]. Song H, Mak KK, Topol L, Yun K, Hu J, Garrett L, Chen Y, Park O, Chang J, Simpson RM, Wang CY, Gao B, Jiang J, Yang Y: Mammalian Mst1 and Mst2 kinases play essential roles in organ size control and tumor suppression. Proc Natl Acad Sci U S A 2010, 107:1431–6. [PubMed: 20080598]

[31]. Kowalik MA, Saliba C, Pibiri M, Perra A, Ledda-Columbano GM, Sarotto I, Ghiso E, Giordano S, Columbano A: Yes-associated protein regulation of adaptive liver enlargement and hepatocellular carcinoma development in mice. Hepatology 2011, 53:2086–96. [PubMed: 21391223]

[32]. Tschaharganeh DF, Chen X, Latzko P, Malz M, Gaida MM, Felix K, Ladu S, Singer S, Pinna F, Gretz N, Sticht C, Tomasi ML, Delogu S, Evert M, Fan B, Ribback S, Jiang L, Brozzetti S, Bergmann F, Dombrowski F, Schirmacher P, Calvisi DF, Breuhahn K: Yes-associated protein up-regulates Jagged-1 and activates the Notch pathway in human hepatocellular carcinoma. Gastroenterology 2013, 144:1530–42 e12. [PubMed: 23419361]

[33]. Wang J, Ma L, Weng W, Qiao Y, Zhang Y, He J, Wang H, Xiao W, Li L, Chu Q, Pan Q, Yu Y, Sun F: Mutual interaction between YAP and CREB promotes tumorigenesis in liver cancer. Hepatology 2013, 58:1011–20. [PubMed: 23532963]

[34]. Perra A, Kowalik MA, Ghiso E, Ledda-Columbano GM, Di Tommaso L, Angioni MM, Raschioni C, Testore E, Roncalli M, Giordano S, Columbano A: YAP activation is an early event and a potential therapeutic target in liver cancer development. J Hepatol 2014, 61:1088–96. [PubMed: 25010260]

[35]. Tao J, Calvisi DF, Ranganathan S, Cigliano A, Zhou L, Singh S, Jiang L, Fan B, Terracciano L, Armeanu-Ebinger S, Ribback S, Dombrowski F, Evert M, Chen X, Monga SPS: Activation of beta-catenin and Yap1 in human hepatoblastoma and induction of hepatocarcinogenesis in mice. Gastroenterology 2014, 147:690–701. [PubMed: 24837480]

[36]. Fitamant J, Kottakis F, Benhamouche S, Tian HS, Chuvin N, Parachoniak CA, Nagle JM, Perera RM, Lapouge M, Deshpande V, Zhu AX, Lai A, Min B, Hoshida Y, Avruch J, Sia D, Camprecios G, McClatchey AI, Llovet JM, Morrissey D, Raj L, Bardeesy N: YAP Inhibition Restores Hepatocyte Differentiation in Advanced HCC, Leading to Tumor Regression. Cell reports 2015.

[37]. Hayashi H, Higashi T, Yokoyama N, Kaida T, Sakamoto K, Fukushima Y, Ishimoto T, Kuroki H, Nitta H, Hashimoto D, Chikamoto A, Oki E, Beppu T, Baba H: An Imbalance in TAZ and YAP Expression in Hepatocellular Carcinoma Confers Cancer Stem Cell-like Behaviors Contributing to Disease Progression. Cancer Res 2015, 75:4985–97. [PubMed: 26420216]

[38]. Xiao H, Jiang N, Zhou B, Liu Q, Du C: TAZ regulates cell proliferation and epithelial-mesenchymal transition of human hepatocellular carcinoma. Cancer Sci 2015, 106:151–9. [PubMed: 25495189]

[39]. Nishio M, Sugimachi K, Goto H, Wang J, Morikawa T, Miyachi Y, Takano Y, Hikasa H, Itoh T, Suzuki SO, Kurihara H, Aishima S, Leask A, Sasaki T, Nakano T, Nishina H, Nishikawa Y, Sekido Y, Nakao K, Shin-Ya K, Mimori K, Suzuki A: Dysregulated YAP1/TAZ and TGF-beta signaling mediate hepatocarcinogenesis in Mob1a/1b-deficient mice. Proc Natl Acad Sci U S A 2016, 113:E71–80. [PubMed: 26699479]

[40]. Sohn BH, Shim JJ, Kim SB, Jang KY, Kim SM, Kim JH, Hwang JE, Jang HJ, Lee HS, Kim SC, Jeong W, Kim SS, Park ES, Heo J, Kim YJ, Kim DG, Leem SH, Kaseb A, Hassan MM, Cha M, Chu IS, Johnson RL, Park YY, Lee JS: Inactivation of Hippo Pathway Is Significantly Associated with Poor Prognosis in Hepatocellular Carcinoma. Clin Cancer Res 2016, 22:1256–64. [PubMed: 26459179]

[41]. Lin C, Hu Z, Lei B, Tang B, Yu H, Qiu X, He S: Overexpression of Yes-associated protein and its association with clinicopathological features of hepatocellular carcinoma: A meta-analysis. Liver Int 2017, 37:1675–81. [PubMed: 28345185]

[42]. Chen R, Zhu S, Fan XG, Wang H, Lotze MT, Zeh HJ 3rd, Billiar TR, Kang R, Tang D: High mobility group protein B1 controls liver cancer initiation through yes-associated protein -dependent aerobic glycolysis. Hepatology 2018, 67:1823–41. [PubMed: 29149457]

[43]. Moya IM, Castaldo SA, Van den Mooter L, Soheily S, Sansores-Garcia L, Jacobs J, Mannaerts I, Xie J, Verboven E, Hillen H, Alguero-Nadal A, Karaman R, Van Haele M, Kowalczyk W, De Waegeneer M, Verhulst S, Karras P, van Huffel L, Zender L, Marine JC, Roskams T, Johnson R, Aerts S, van Grunsven LA, Halder G: Peritumoral activation of the Hippo pathway effectors YAP and TAZ suppresses liver cancer in mice. Science 2019, 366:1029–34. [PubMed: 31754005]

[44]. Bruschi FV, Tardelli M, Einwallner E, Claudel T, Trauner M: PNPLA3 I148M Up-Regulates Hedgehog and Yap Signaling in Human Hepatic Stellate Cells. Int J Mol Sci 2020, 21.

[45]. Huang H, Tsui YM, Ng IO: Fueling HCC Dynamics: Interplay Between Tumor Microenvironment and Tumor Initiating Cells. Cell Mol Gastroenterol Hepatol 2023, 15:1105–16. [PubMed: 36736664]

[46]. Brouillet A, Lafdil F: Risk factors of primary liver cancer initiation associated with tumour initiating cell emergence: novel targets for promising preventive therapies. eGastroenterology 2023, 1:e100010. [PubMed: 39944247]

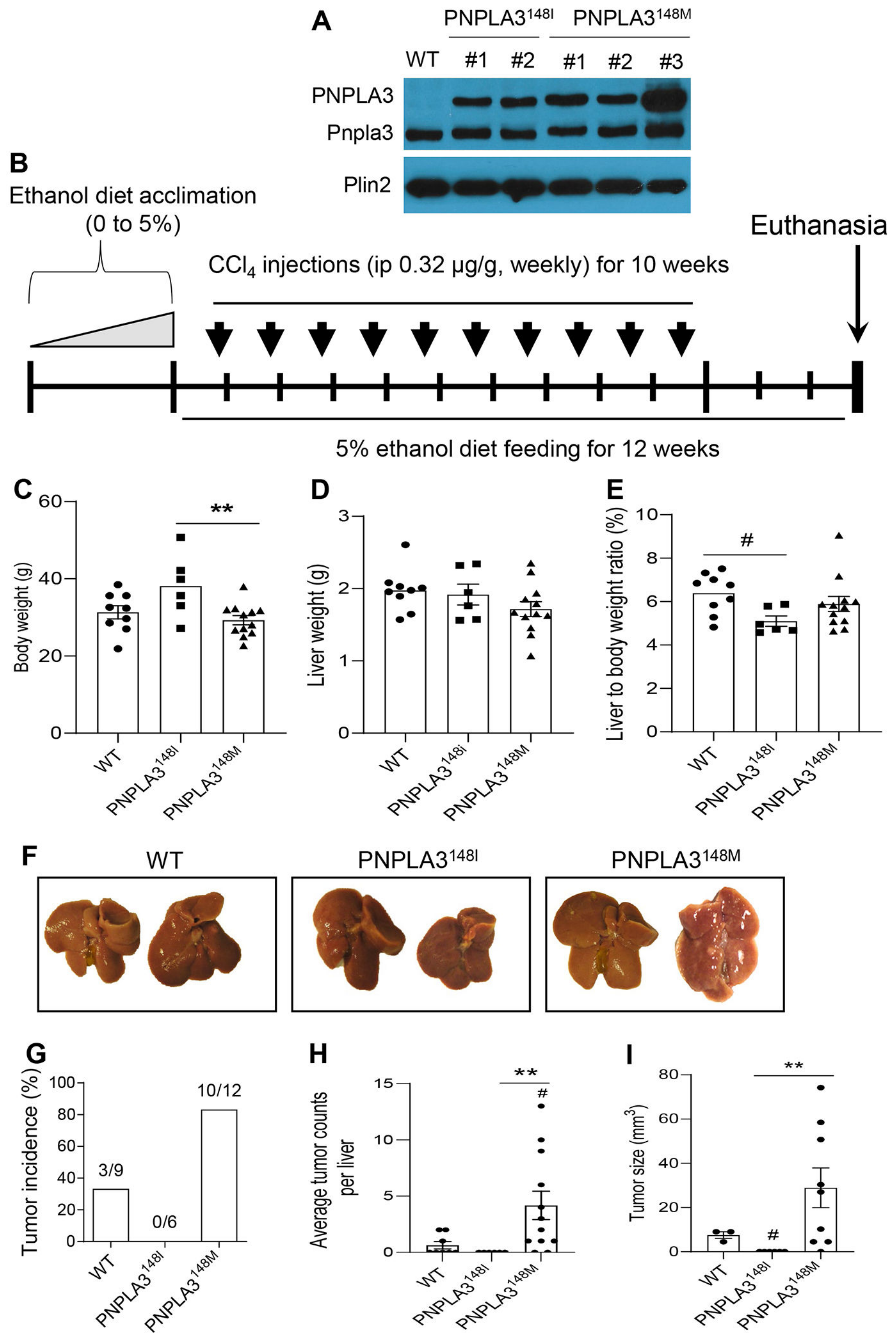

Figure 1. PNPLA3^{148M} promotes liver cancer in an ethanol-fed mouse model.

(A) Verification of human PNPLA3 transgenic mice by Western blot analysis. (B) Schematic diagram of the mouse model used for this study. WT, PNPLA3^{148I}, and PNPLA3^{148M} mice were fed with a 5% (vol/vol) ethanol-containing diet for 12 weeks plus weekly CCl_4 injections (0.32 μg/g, i.p.) for 10 weeks. (C-E) Body and liver weight measurements. (F) Mouse liver gross images. (G-I) Liver cancer incidence rates, tumor counts, and tumor sizes, respectively. Data were expressed as mean ± SEM. $^{\#}P < 0.05$ for WT vs. other groups; $^{**}P < 0.01$ for PNPLA3^{148M} vs. PNPLA3^{148I} (n = 6-12).

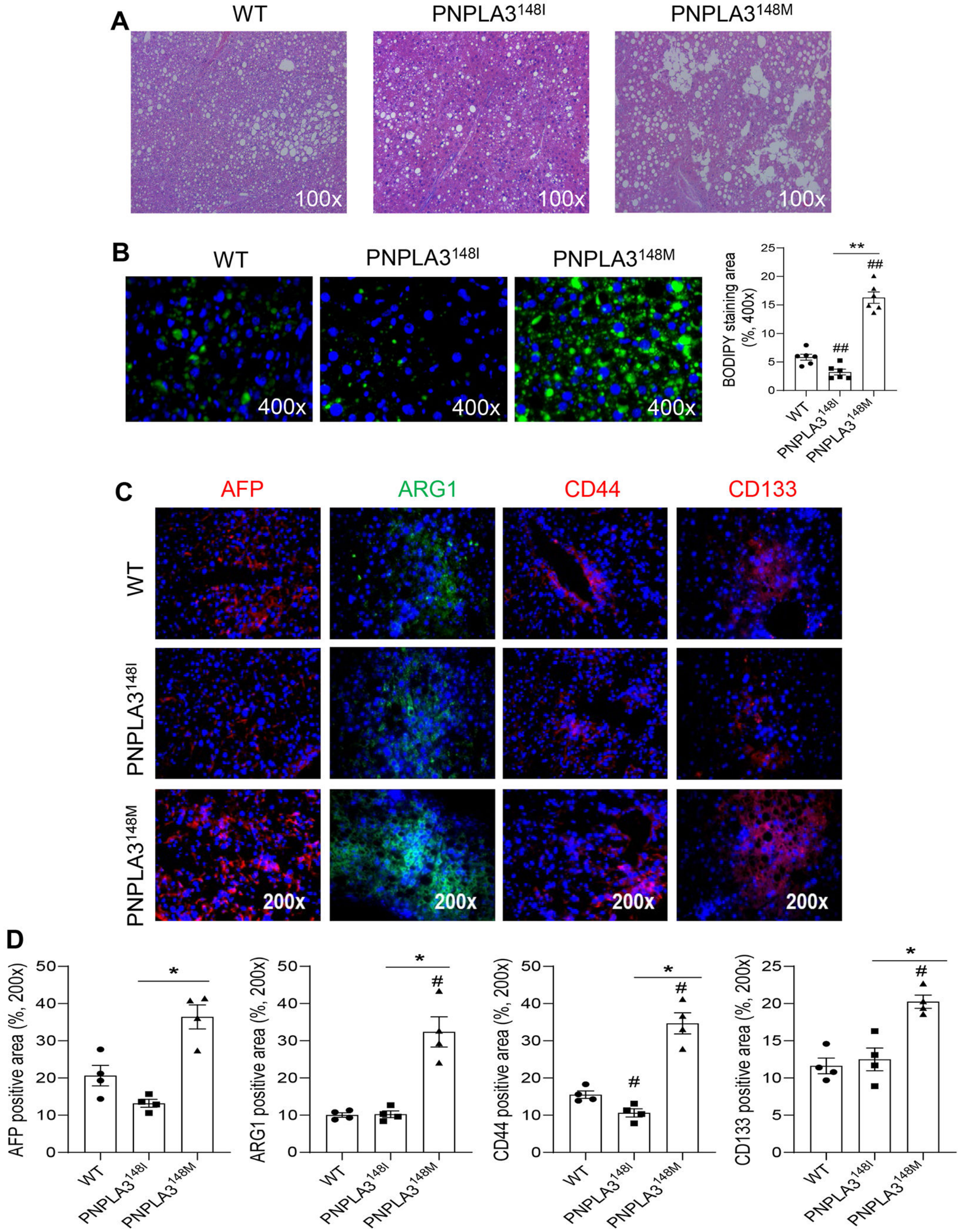

Figure 2. Characterization of hepatocellular carcinoma.

(A) Representative H&E staining of liver sections. (B) Lipid droplet analysis by BODIPY staining. (C, D) Immunofluorescence and quantification analysis of AFP, ARG1, CD44, and CD133 in liver sections. Total magnification of the images was labeled as such (100x, 200x, or 400x). Data were expressed as mean ± SEM. $^{\#}P < 0.05$ and $^{\#\#}P < 0.01$ for WT vs. other groups; $^{*}P < 0.05$ and $^{**}P < 0.01$ for PNPLA3^{148M} vs. PNPLA3^{148I} (n = 4).

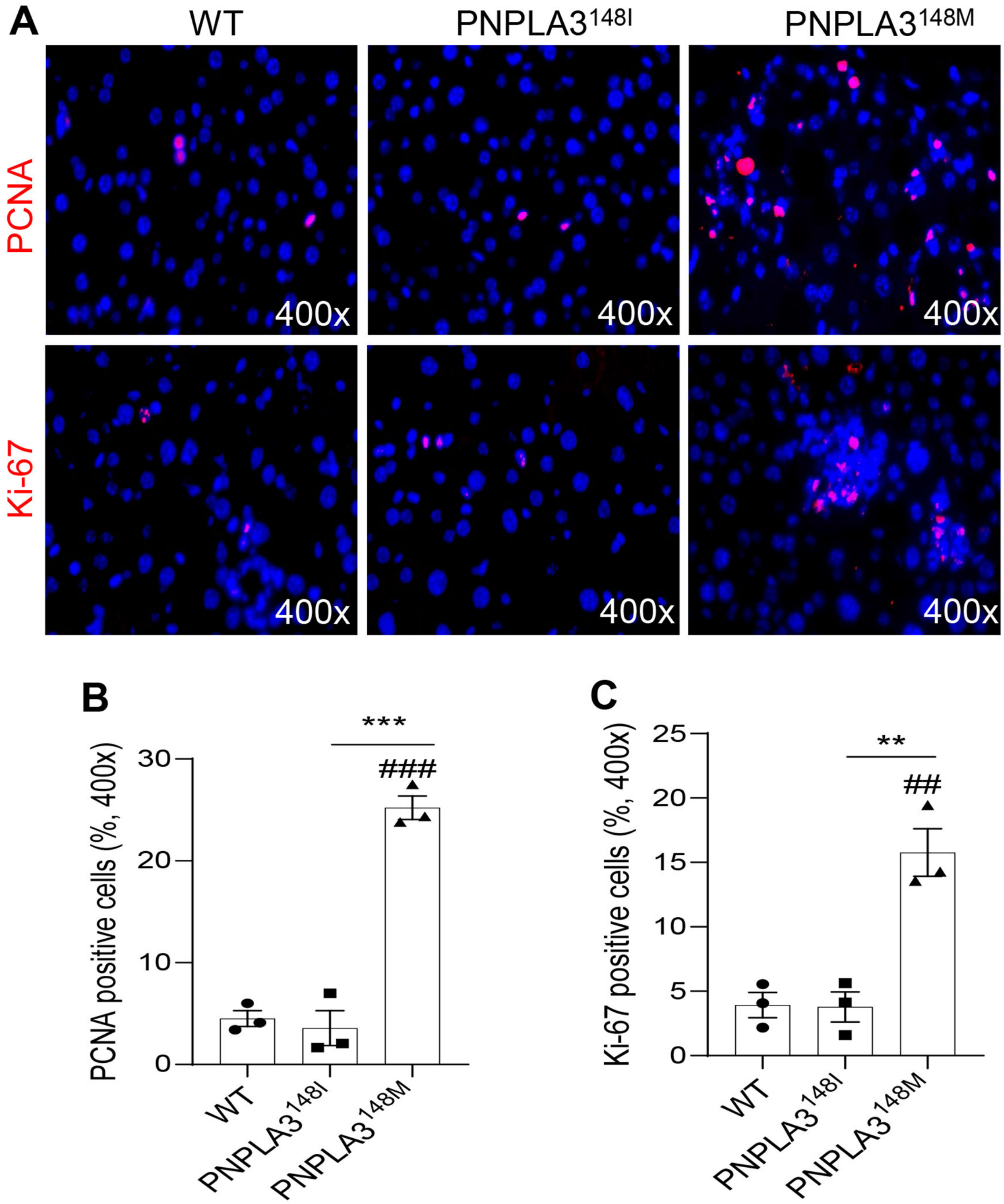

Figure 3. Cell proliferation is increased in the liver of PNPLA3^{148M} mice.

(A-C) Immunofluorescence and quantification analysis of PCNA and Ki-67 in liver sections. Total magnification of the images was 400x. Data were expressed as mean ± SEM. $^{\#\#}P < 0.01$ and $^{\#\#\#}P < 0.001$ for PNPLA3^{148M} vs. WT; $^{**}P < 0.01$ and $^{***}P < 0.001$ for PNPLA3^{148M} vs. PNPLA3^{148I} (n = 3).

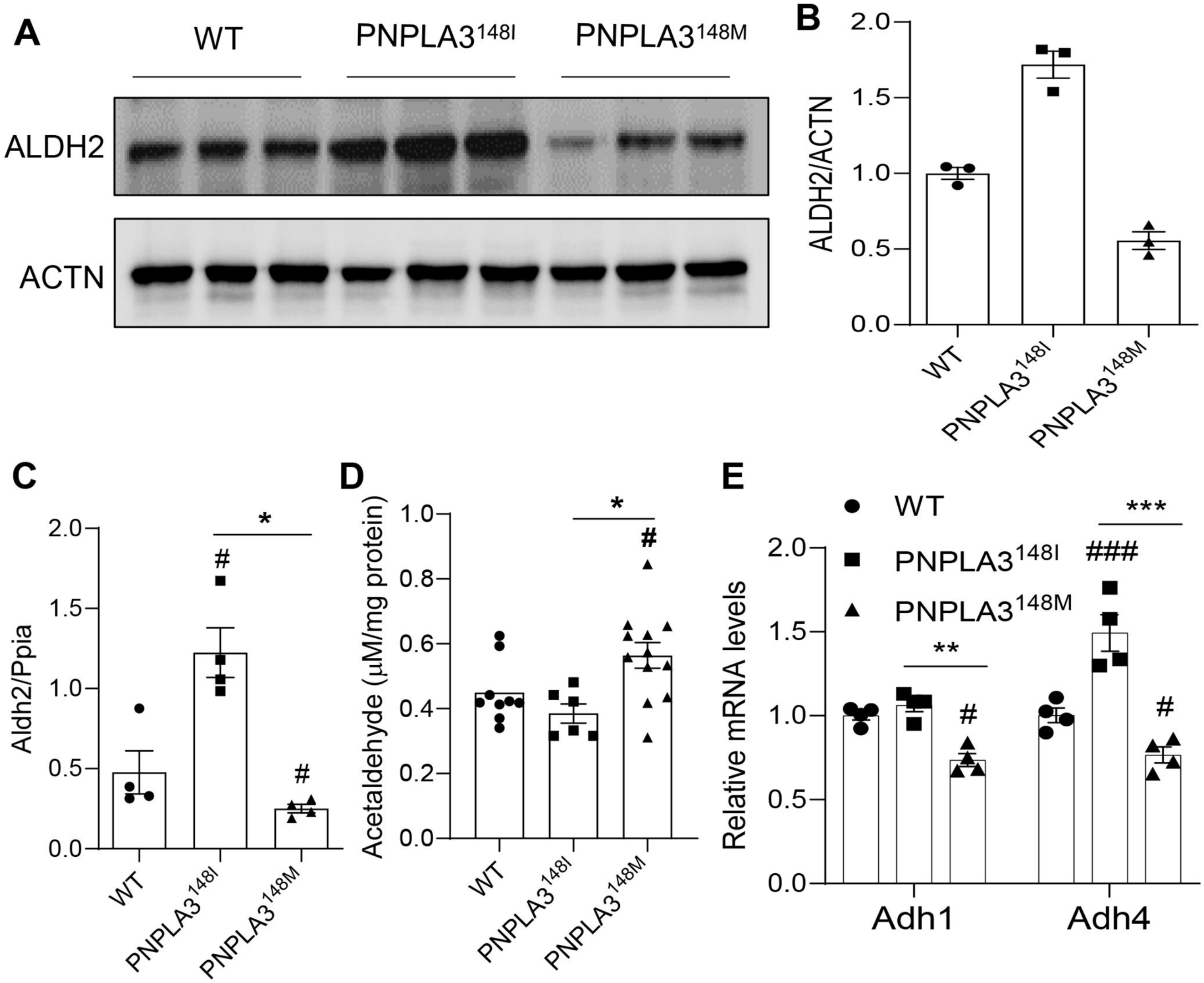

Figure 4. PNPLA3^{148M} impairs ethanol detoxification.

(A, B) Hepatic ALDH2 protein analysis (n = 3). (C) Aldh2 mRNA analysis by real-time PCR (n = 4). (D) Hepatic acetaldehyde measurements (n = 6-11). (E) Adh1 and Adh4 mRNA analysis by real-time PCR. Data were expressed mean ± SEM. $^{\#}P < 0.05$ and $^{\#\#\#}P < 0.001$ for WT *vs*. other groups; $^{*}P < 0.05$, $^{**}P < 0.01$, and $^{***}P < 0.001$ for PNPLA3^{148I} *vs.* PNPLA3^{148M}.

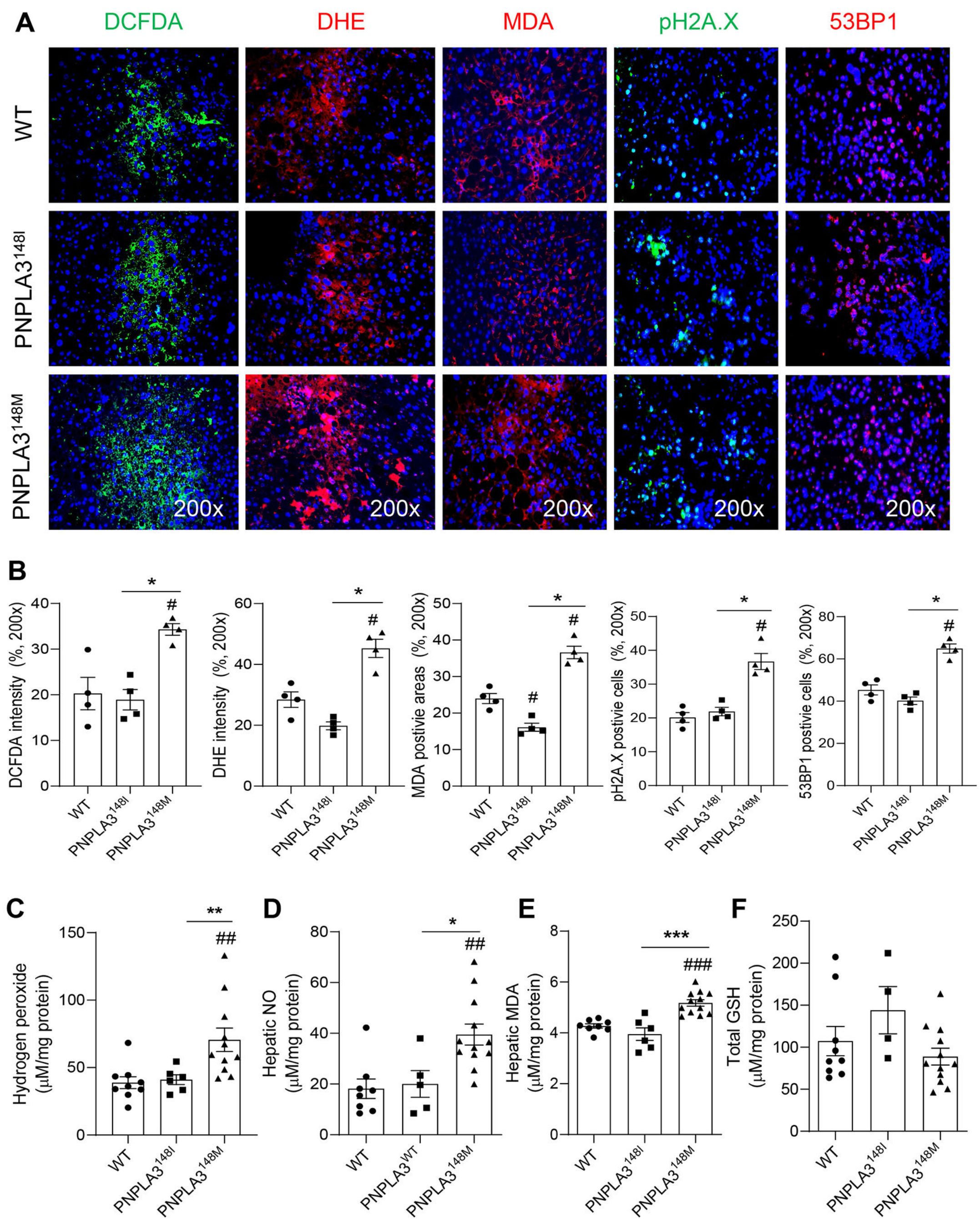

Figure 5. PNPLA3^{148M} exacerbates ethanol-induced oxidative stress and DNA damage.

(A, B) Fluorescence imaging analysis of DCFDA, DHE, MDA, pH2A.X, and 53BP1 in liver sections. Total magnification of the images was 200x. (C-F) Hepatic hydrogen peroxide, nitric oxide (NO), MDA, and total glutathione (GSH) measurements (n = 6-12), respectively. Data were expressed mean ± SEM. $^{\#}P < 0.05$, $^{\#\#}P < 0.01$, and $^{\#\#\#}P < 0.001$ for WT *vs.* other groups; *P<0.05, **P<0.01, and ***P<0.001 for PNPLA3^{148I} *vs.* PNPLA3^{148M}.

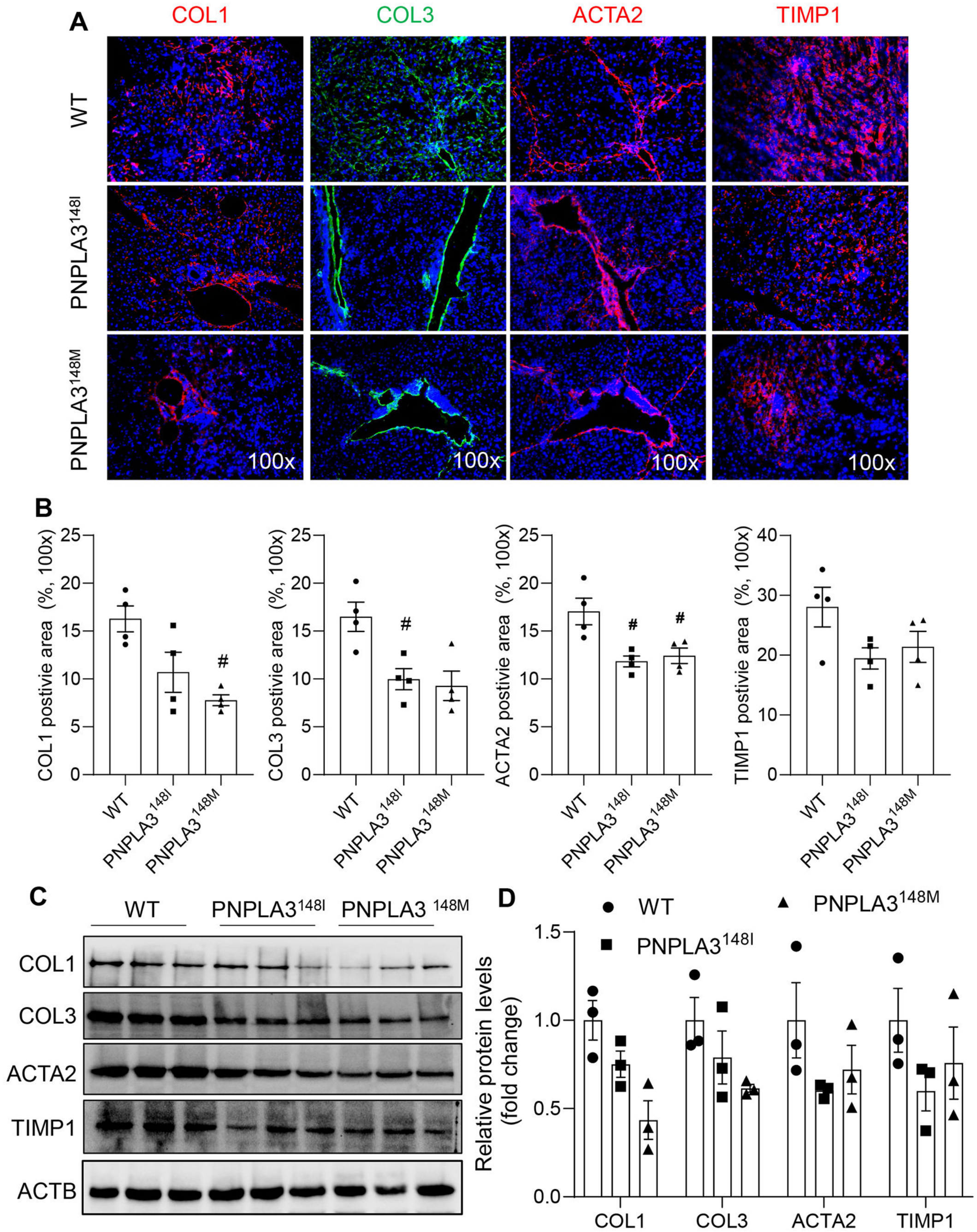

Figure 6. Extracellular matrix (ECM) protein analysis in the PNPLA3^{148M} mouse livers.

(A, B) Immunofluorescence analysis of COL1, COL3, ACTA2, and TIMP1 in liver sections (n = 4). Total magnification of the images was 100x. (C, D) Western blot analysis of ECM related proteins in liver tissues (n = 3). Data were expressed mean ± SEM. $^{\#}P < 0.05$ for WT *vs.* other groups.

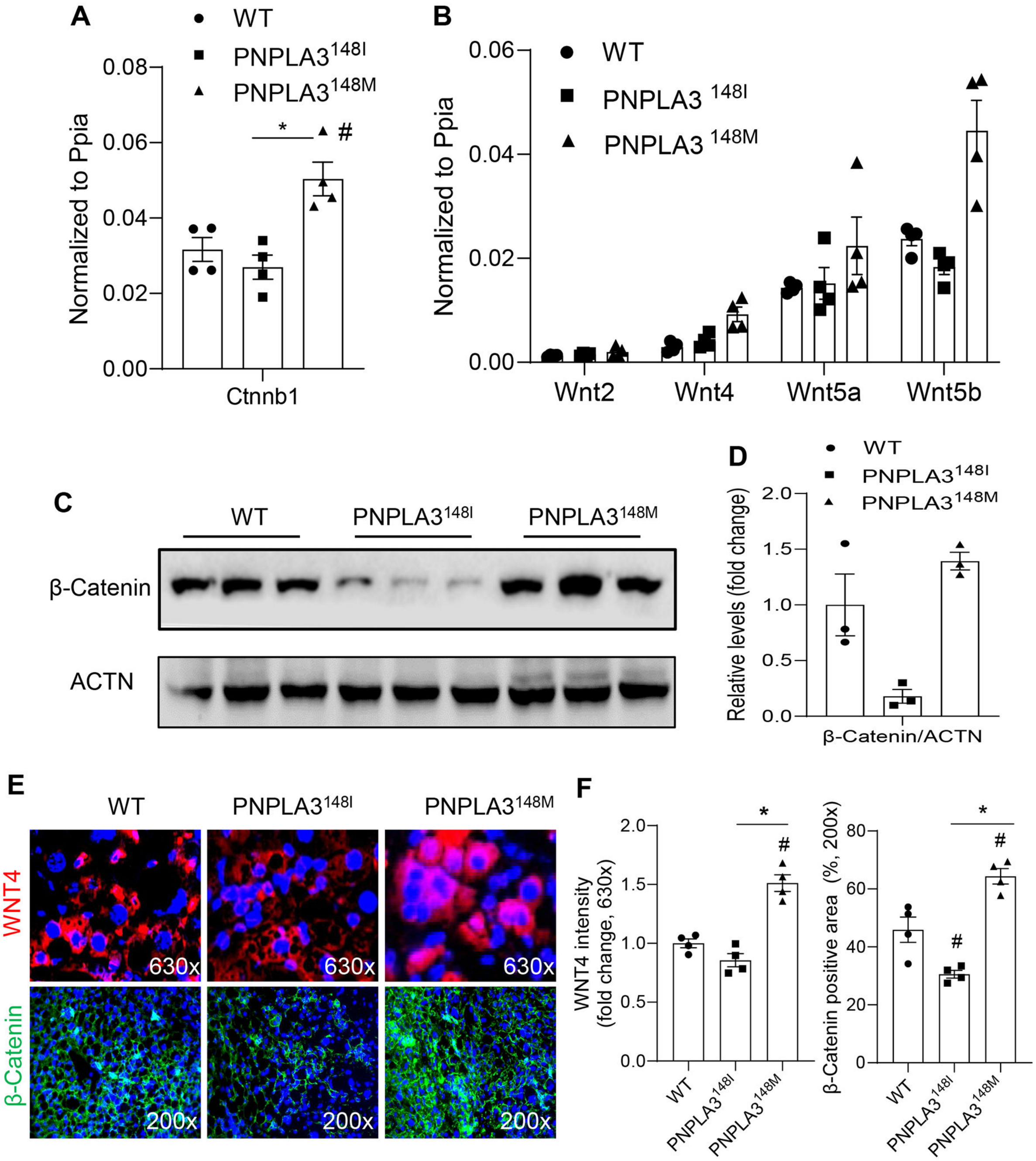

Figure 7. The Wnt/β-catenin pathway is elevated in the PNPLA3^{148M} mouse livers.

(A, B) Real-time PCR analysis of *Ctnnb1* and *Wnt* gene expression (n = 4). (C, D) Western blot analysis of β-catenin in mouse liver lysates (n = 3). (E, F) Immunofluorescence imaging analysis of Wnt4 and β-catenin in the liver sections (n = 4). Total magnification of the images was labeled as such (630x or 200x). Data were expressed mean ± SEM. $^{\#}P < 0.05$ for WT *vs.* other groups; $^{*}P < 0.05$ for PNPLA3^{148I} *vs.* PNPLA3^{148M}.

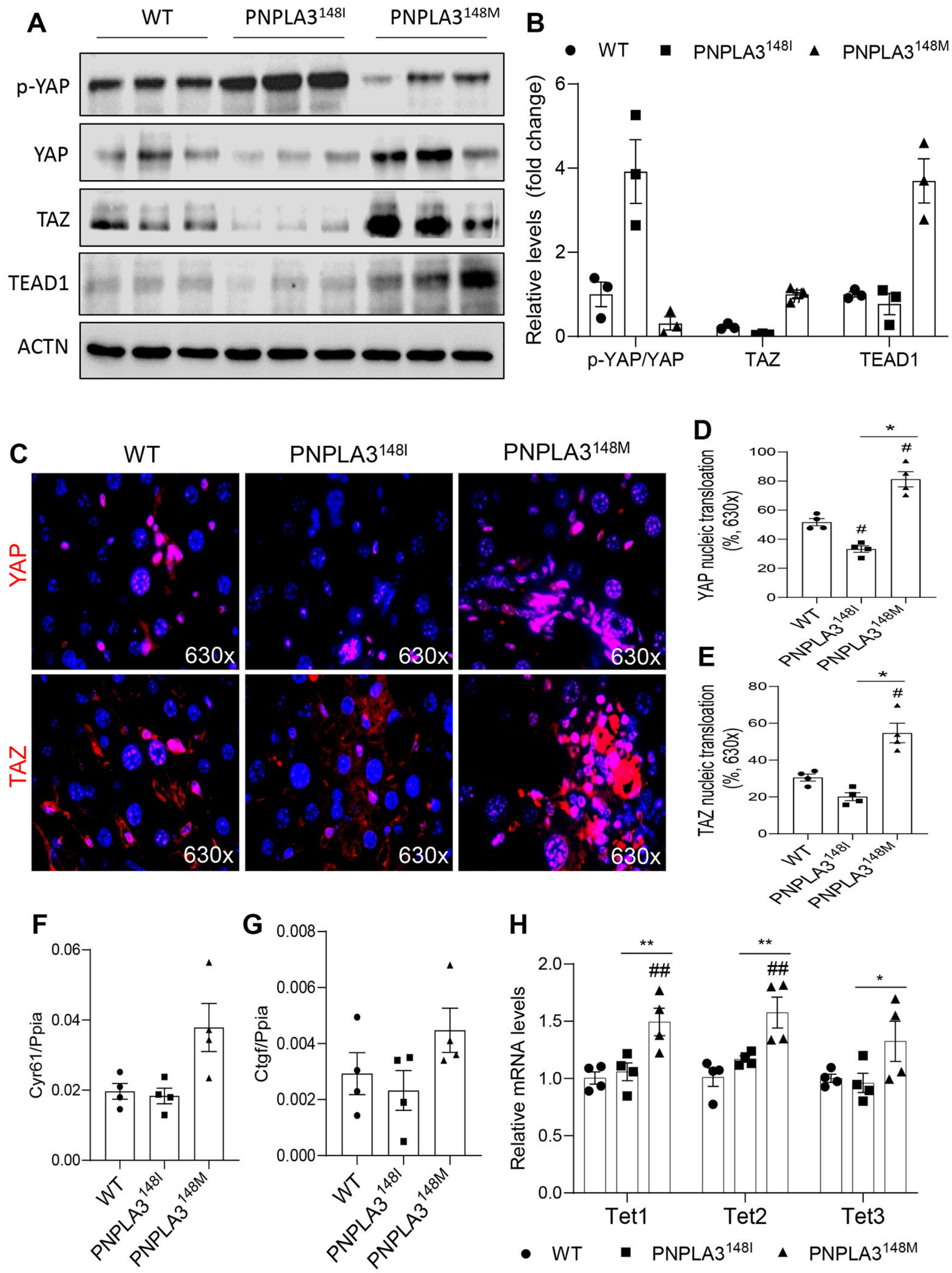

Figure 8. YAP/TAZ are activated in the PNPLA3^{148M} mouse livers.

(A, B) Western blot analysis p-YAP, YAP, TAZ, and TEAD1 in liver lysates (n = 3). (C-E) Immunofluorescence imaging analysis of YAP and TAZ in liver sections (n = 4). Total magnification of the images was 630x. (F-H) Real-time PCR analysis of Cyr61, Ctgf, and Tet1/2/3 mRNA levels (n = 4). Data were expressed mean ± SEM. $^{\#}P < 0.05$ and $^{\#\#}P < 0.01$ for WT *vs*. other groups; $^{*}P < 0.05$ and $^{**}P < 0.01$ for PNPLA3^{148I} *vs*. PNPLA3^{148M}.

Table 1.

PCR primer sequences

Gene symbol	Species	Primer sequences (forward and reverse)	Application
Aldh2	Mouse	5′- TGA TCA AGG AGG CAG GCT TT-3′ 5′- CCA CTT TGT CCA CAC CCT CA-3′	qPCR
Ctnnb1	Mouse	5′- TCA GTG CAG GAG GCC GA-3′ 5′- CAG GTC AGC TTG AGT AGC CAT-3′	qPCR
Wnt2	Mouse	5′- GTC TGA CCT GAT GTA GAC GCA-3′ 5′- CTG TAG CTC TCA TGT ACC ACC AT-3′	qPCR
Wnt4	Mouse	5′- CAG AGC CAC ATG CTC CTA GA-3′ 5′- TCA CGT CCT GAT AGG CAC AG-3′	qPCR
Wnt5a	Mouse	5′-CAA GGA GTT CGT GGA CGC TA-3′ 5′-CAG GCT ACA TCT GCC AGG TT-3′	qPCR
Wnt5b	Mouse	5′- GTG CCA ACA CCA GTT TCG AC-3′ 5′- GAA GGC AGT CTC TCG GCT AC-3′	qPCR
Cyr61	Mouse	5′- AGA GGC TTC CTG TCT TTG GC-3′ 5′- CCA AGA CGT GGT CTG AAC GA-3′	qPCR
Ctgf	Mouse	5′- TGC AGA CTG GAG AAG CAG AG-3′ 5′- GGC TTG GCG ATT TTA GGT GT-3′	qPCR
Adh1	Mouse	5′- GGA GCT TCA CCA CTG GAC AA-3′ 5′- GGT CAC CTT GGC GAC TTT GA-3′	qPCR
Adh4	Mouse	5′- GCC AGA GTC GAT GAT GAG GC-3′ 5′- CAG GCC AAA GAC AGC ACA AG-3′	qPCR
Tet1	Mouse	5′- CTG CTG TCA GGG AGC TCA TG-3′ 5′- GAG CTC TTC CCT TCC TTC CC-3′	qPCR
Tet2	Mouse	5′- GGC AAG AGC TCT CAG GGA TG-3′ 5′- AGG TCG CAC TCG TAC CAA AC-3′	qPCR
Tet3	Mouse	5′- TAC CCT CCG GAA GTA TGG CA-3′ 5′- TAC ATG CTC CAG GAA CAG CC-3′	qPCR